Nanoscale backswitched domain patterning in lithium niobate

V. Ya. Shur,[a] E. L. Rumyantsev, E. V. Nikolaeva, E. I. Shishkin, and D. V. Fursov
Institute of Physics and Applied Mathematics, Ural State University, Ekaterinburg 620083, Russia

R. G. Batchko, L. A. Eyres, M. M. Fejer, and R. L. Byer
E.L. Ginzton Laboratory, Stanford University, Stanford, California 94305

(Received 29 July 1999; accepted for publication 11 November 1999)

We demonstrate a promising method of nanoscale domain engineering, which allows us to fabricate regular nanoscale domain patterns consisting of strictly oriented arrays of nanodomains (diameter down to 30 nm and density up to 100 μm^{-2}) in lithium niobate. We produce submicron domain patterns through multiplication of the domain spatial frequency as compared with the electrode one. The fabrication techniques are based on controlled backswitched poling. © *2000 American Institute of Physics.* [S0003-6951(00)01402-9]

In recent years, domain engineering, as a new branch of technology connected with fabrication of periodic ferroelectric domain structures with desirable parameters, is rapidly developing. Its advance is a critical step in the manufacturing of electro-optical[1] and nonlinear optical devices.[2–5] Engineerable nonlinear optical materials have permitted the development of a wide range of tunable coherent light sources based on quasiphase matching.[6] Lithium niobate is widely used due to its large electro-optical and nonlinear optical coefficients.[7] Application of an electric field through lithographically defined electrodes for domain patterning is one of the most promising methods.[8] However, high coercive electric fields and the strong effect of domain widening out of the electroded area impose limitations on the period of short-pitch domain patterns. Up to now, domain patterns with periods less than 1 μm have not been fabricated. In this work, we report an approach which allows to us overcome this obstacle.

Periodic domain structures were obtained in standard optical-grade single-domain 0.5-mm-thick $LiNbO_3$ wafers of congruent composition cut perpendicular to the polar axis. The wafers were photolithographically patterned with a periodic stripe metal–electrode structure (NiCr) deposited on a $\mathbf{Z}^+$ surface and oriented along the **Y** axis. The patterned surface was covered by a thin (about 0.5-mm-thick) insulating layer (photoresist) [Fig. 1(a)]. A high-voltage pulse producing an electric field greater than the coercive field for quasistatic switching ($E_c = 21.5$ kV/mm) was applied to the structure through a fixture containing liquid electrolyte (LiCl).[9,10] The wave form for backswitched poling consisted of three levels of external field: ''high field,'' ''low field'' and ''stabilization field,'' [Fig. 1(b)]. The switching from the single-domain state took place at the ''high field'' and the backswitching (flip-back)[11–13] occurred at the ''low field.'' The crucial parameters for backswitching kinetics were the duration of the ''high-field'' stage Δt_{sp} and the field-diminishing amplitude ΔE. The domain patterns obtained for different durations of the ''low field'' stage yielded information about the domain structure development during backswitching. For observation of the domain patterns after partial poling, the **Z** surfaces and polished **Y** cross sections were etched for 5–10 min by hydrofluoric acid without heating.[10] The obtained surface relief was visualized by optical microscope, scanning electron microscopy (SEM), and atomic force microscopy (AFM), techniques.

Distinguishable stages of domain evolution have been observed during backswitched poling.[11–13] The process starts with nucleation (arising of new domains) at the $\mathbf{Z}^+$ polar surface along the electrode edges [Fig. 2(a)]. During the second stage, these domains grow and propagate through the sample. As a result of merging, laminar domains with plane walls are formed. Pronounced domain broadening out of the electroded area is always observed [Fig. 2(b)]. After rapid decreasing of the poling field, the backswitching starts through shrinking of the laminar domains by the backward wall motion and nucleation along the electrode edges [Fig. 2(c)]. We have shown that various regular nanodomain structures can be produced by backswitched poling by presetting the voltage wave-form parameters. The types of domain patterns depend also on the value of the domain-wall shift out of the electrodes.

Backswitched domain frequency multiplication. For small domain-wall shift out of electrodes, we have revealed a backswitched effect—multiplication of the domain pattern

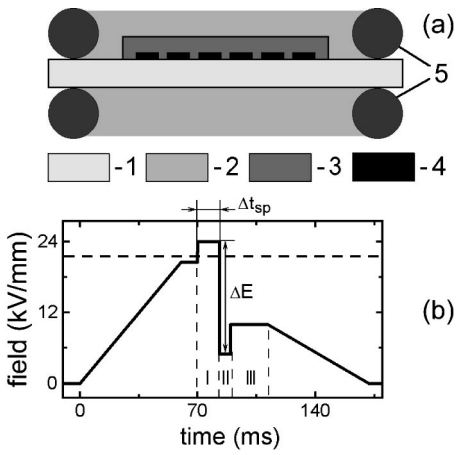

FIG. 1. (a) Scheme of the experimental setup and (b) backswitched poling voltage waveform.

[a]Electronic mail: vladimir.shur@usu.ru

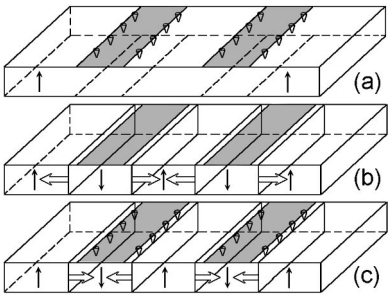

FIG. 2. Stages of domain evolution during backswitched poling. White arrows: directions of domain-wall motion.

frequency as compared to the electrode one. The mechanism of frequency multiplication is based on the nucleation along the electrode edges during backswitching, while the role of the wall motion in this case is negligible. For ''frequency tripling'' [Fig. 3(c)], the subsequent growth and merging of nucleated domains lead to formation of a couple of strictly oriented sub-micron-width domain stripes under each electrode. Their depth is about 20–50 μm [Fig. 3(d)]. It is clear that this structure can be produced only by using wide enough electrodes. For narrow electrodes these stripes merge and only the ''frequency doubling'' can be obtained [Fig. 3(a)]. The depth of these backswitched domain stripes is, typically, about 50–100 μm [Fig. 3(b)].

The backswitched domain cross sections reveal two distinct variants of domain evolution during frequency multiplication: ''erasing'' and ''splitting.'' During ''erasing,'' backswitched domains are formed in the earlier switched area without variation of the external shape of the switched laminar domains [Fig. 3(e)]. During ''splitting,'' the backswitched domains cut the initial ones conserving its volume [Fig. 3(f)].

More complicated frequency multiplication is demonstrated for sufficient domain spreading out of electrodes during switching. For long switching pulse $\Delta t_{sp} \sim 15$ ms and large field-diminishing amplitude $\Delta E \sim 20$ kV/mm [Fig. 1(b)], the backswitching also starts with the formation of the couple of arrays under the electrode edges [Fig. 4(a)]. Then, the arrays turn into a pair of stripe domains through growth and merging of individual domains [Fig. 4(b)]. Surprisingly, after complete merging the secondary couple of arrays appear in the nonelectroded area parallel to the initial ones [Fig. 4(c)]. This self-maintaining process leads to the formation of periodic stripe domains oriented along the electrodes

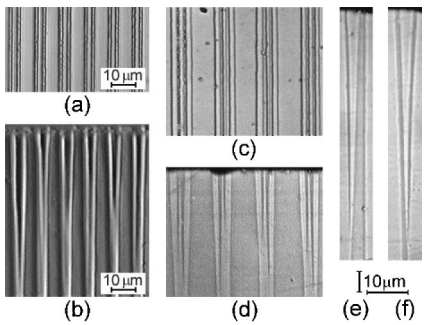

FIG. 3. Backswitched domain frequency multiplication. (a) and (b) ''frequency doubling;'' (c) and (d) ''frequency tripling;'' (e) ''erasing;'' (f) ''splitting.'' (a) and (c) $\mathbf{Z}^+$ view; and (b), (d), (e), and (f) **Y** cross sections.

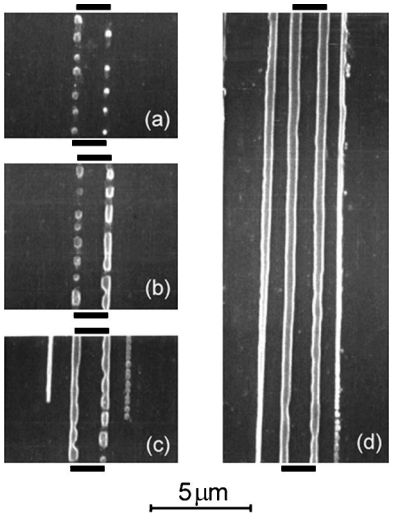

FIG. 4. SEM patterns demonstrating the stages of the formation of periodic stripe domains along the electrode edges. $\mathbf{Z}^+$ view. Electrodes cover the area between the black rectangles. Electrodes are oriented along the **Y** direction.

[Fig. 4(d)]. The distance between the secondary and initial stripes is about the thickness of the insulating layer.

Formation of the regular nanodomain structures. For sufficient domain spreading out of electrodes, but for short switching pulse duration $\Delta t_{sp} \sim 5$ ms and small field-diminishing amplitude $\Delta E \sim 2$ kV/mm, the backswitched domain evolution is changed drastically and represents self-maintained self-organized growth of oriented nanoscale domain arrays. The domain patterns revealed by etching and visualized by SEM demonstrate the array-assisted reversal motion of the existing domain walls through propagation of the highly organized quasiperiodical structure of domain arrays strictly oriented along crystallographic directions (Fig. 5). Each quasiregular array is comprised of nanodomains with a diameter of 30–100 nm and an average linear density exceeding 10^4 mm^{-1}.

Two variants of array orientation are obtained. In the usual case, all nanodomain arrays are strictly oriented along the $\mathbf{Y}^-$ direction at 60° to the electrode edges [Fig. 5(a)]. A similar oriented nucleation has been observed during polarization reversal in strong homogeneous fields.[14,15] In some cases the domain arrays are strictly oriented along the $\mathbf{X}^-$ or $\mathbf{X}^+$ directions [Fig. 5(b)], and individual nanodomains have a triangular shape. There are four equal **X** directions oriented at 30° to the electrode edges. So, the domain pattern consisting of regular 30° array fragments with different array orientations are obtained along one domain wall [Fig. 5(c)]. The array patterns growing along the **X** directions at 90° to the electrodes are different, as the fast growth of nanodomains along the electrodes leads to the formation of a periodic set of nanoscale stripe domains with a period less than 60 nm [Fig. 5(d)].

All effects observed during backswitching can be explained by the nonuniform distribution of the local backswitching field near the electrode edges and domain walls due to spatially nonuniform screening of the external and depolarization fields.[16] Our estimations reveal the field maximum at a distance about the thickness of the insulating layer from the domain wall or nanodomain array.[15] An array ag-

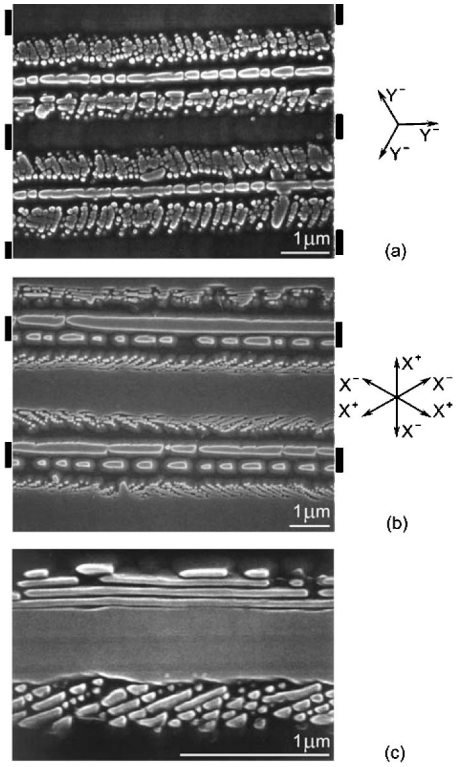

FIG. 5. SEM nanodomain patterns with arrays oriented along different axes: (a) $\mathbf{Y}^{-}$ at 60° to the electrode edges, (b) **X** at 30° and 90° to the electrode edges, and (c) coexistence of different array orientations. $\mathbf{Z}^{+}$ view. Electrodes cover the area between the black rectangles. Electrodes are oriented along the **Y** direction.

gregate existing at a given moment generates the new maximum of the backswitching field at a fixed distance in front of its boundary and triggers the arising of the new array. The developing correlated nucleation leads to the self-maintaining generation of the parallel arrays. The array-assisted propagation of the correlated domain structure is similar to the formation of the ''wide domain boundary'' discovered in $Pb_5Ge_3O_{11}$ during switching in ''super-strong'' fields.[17]

We demonstrate promising possibilities in domain engineering based on backswitched poling. The multiplication of the domain spatial frequency as compare with the electrode one allows us to produce domain structures with submicron periods. Quasiregular patterns of oriented arrays of nanoscale domains (with a density up to $100\,\mu\mathrm{m}^{-2}$) were fabricated. The proposed method of domain engineering can be used in a wide range of applications and for manufacturing of various devices.

This material is based upon work partially supported by the Program ''Basic Research in Russian Universities'' under Grant No. 5563, by the EOARD, Air Force Office of Scientific Research, Air Force Research Laboratory, under Contract No. F61775-99-WE037, and by DARPA/ONR through the Center of Nonlinear Optical Materials (CNOM) at Stanford University under ONR Grant No. 00014-92-J-1903 and LLNL.

[1] M. Yamada, M. Saitoh, and H. Ooki, Appl. Phys. Lett. **69**, 3659 (1996).
[2] D. Feng, N. B. Ming, J. F. Hong, Y. S. Yang, J. S. Zhu, Z. Yang, and Y. N. Wang, Appl. Phys. Lett. **37**, 607 (1980).
[3] N. B. Ming, J. F. Hong, and D. Feng, J. Mater. Sci. **17**, 1663 (1982).
[4] A. Feisst and P. Koidl, Appl. Phys. Lett. **47**, 1125 (1985).
[5] R. L. Byer, J. Nonlinear Opt. Phys. Mater. **6**, 549 (1997).
[6] K. C. Burr, C. L. Tang, M. A. Arbore, and M. M. Fejer, Appl. Phys. Lett. **70**, 3341 (1997).
[7] A. M. Prokhorov and Y. S. Kuzminov, *Physics and Chemistry of Crystalline Lithium Niobate* (Adam Hilger, Bristol, 1990), p. 263.
[8] M. Yamada, N. Nada, M. Saitoh, and K. Watanabe, Appl. Phys. Lett. **62**, 435 (1993).
[9] L. E. Myers, R. C. Eckardt, M. M. Fejer, R. L. Byer, and W. R. Bosenberg, Opt. Lett. **21**, 591 (1996).
[10] G. D. Miller, R. G. Batchko, M. M. Fejer, and R. L. Byer, Proc. SPIE **2700**, 34 (1996).
[11] V. Ya. Shur, R. G. Batchko, E. L. Rumyantsev, G. D. Miller, M. M. Fejer, and R. L. Byer, Proc. 11th ISAF, Piscataway, IEEE, NJ (1999), pp. 399.
[12] V. Shur, E. Rumyantsev, R. Batchko, G. Miller, M. Fejer, and R. Byer, Ferroelectrics **221**, 157 (1999).
[13] R. G. Batchko, V. Ya. Shur, M. M. Fejer, and R. L. Byer, Appl. Phys. Lett. **75**, 1673 (1999).
[14] V. Ya. Shur, E. L. Rumyantsev, R. G. Batchko, G. D. Miller, M. M. Fejer, and R. L. Byer, Phys. Solid State **41**, 1681 (1999).
[15] V. Ya. Shur, E. L. Rumyantsev, E. V. Nikolaeva, E. I. Shishkin, R. G. Batchko, L. A. Eyres, M. M. Fejer, and R. L. Byer, Phys. Rev. Lett. (in press).
[16] V. Ya. Shur, E. V. Nikolaeva, E. L. Rumyantsev, E. I. Shishkin, A. L. Subbotin, and V. L. Kozhevnikov, Ferroelectrics **222**, 323 (1999).
[17] V. Ya. Shur, A. L. Gruverman, N. Yu. Ponomarev, and N. A. Tonkachyova, Ferroelectrics **126**, 371 (1992).